

# EICO measurements of inner-core excited mixed rare-gas clusters

## Direct observation of charge transfer

K. Nagaya<sup>a</sup>, H. Murakami, H. Iwayama, Y. Ohmasa, and M. Yao

Department of Physics, Graduate School of Science, Kyoto University, 606-8502 Kyoto, Japan

Received 24 July 2006 / Received in final form 20 November 2006

Published online 24 May 2007 – © EDP Sciences, Società Italiana di Fisica, Springer-Verlag 2007

**Abstract.** The spectra of deep inner-core excited mixed rare-gas clusters were recorded by using electron ion coincidence (EICO) and multi-hit momentum imaging (MHMI) techniques. The EICO spectra for Ar<sub>99</sub>Kr<sub>1</sub> clusters reveal that singly charged ions are emitted from the inner-core excited clusters in addition to the multiple charged ions. The dependence of the EICO spectra on photon energy and cluster size suggests that the holes created through vacancy cascade on the krypton atoms are transferred to the surrounding atoms, and that the singly charged ions are the primary product of the krypton photoabsorption. Charge localization is suggested for the inner-core excited mixed rare-gas clusters from the analysis of the EICO peak width. The MHMI measurements give us direct evidence for the strong charge migration from X-ray absorbing atoms to surrounding atoms. The photon energy dependence of the PSD image for fragment ions suggests that the momentum of the fragment ions depends on the number of charges generated by the vacancy cascade.

**PACS.** 36.40.-c Atomic and molecular clusters – 36.40.Qv Stability and fragmentation of clusters – 36.40.Wa Charged clusters

## 1 Introduction

The advent of third-generation synchrotron sources has prompted the study of core level excitation of free clusters, and considerable efforts have been devoted to studying the rare-gas clusters by utilizing soft X-ray [1–6]. One of the most fascinating findings among them is that the excitation and de-excitation processes depend not only on the cluster size but also on the atomic site within the cluster [5,6].

Deep inner-core excitation by hard X-ray is a potential probe for studying the atomic scale properties of clusters. By irradiating with hard X-ray, a multiple charged ion is generated in the cluster, and the charges then disperse from the absorbing atom to the surrounding atoms. The multiple charged cluster becomes unstable due to a Coulomb repulsive force, and the fragment ions with different charge to mass ratios are emitted from the cluster (Coulomb explosion) [7,8]. Here, the average size of the fragments and the kinetic energy of the fragment ions are expected to reflect the charge dynamics within the clusters. In addition to the localized character of excitation, deep inner-core excitation enables us to select an X-ray absorbing atom by varying the X-ray energy near the ionization threshold.

In the present study, the de-excitation processes of the inner-core excited mixed rare-gas clusters containing krypton have been studied by using two experimental methods. One of these methods is electron ion coincidence (EICO) measurement, and the other is multi-hit momentum imaging (MHMI). EICO has been utilized to study the cluster size dependence of the de-excitation processes in a mixed cluster. MHMI gives us information on the details of fragmentation dynamics because it can record multiple ion fragments and their space distribution.

## 2 Experimental

The EICO and MHMI measurements were carried out at the high-brilliance undulator beamline BL37XU in SPring8, where the X-ray emitted from the undulator was monochromatized by Si(111) double crystals [9]. The X-ray photon flux was about  $5.4 \times 10^{12}$  photons/s at  $h\nu = 14.50$  keV. The X-ray beam was directed into the cluster beam apparatus [10] through a beryllium window. The cluster beam apparatus consists of two vacuum chambers, an expansion chamber, and an analyzing chamber. Each chamber was evacuated by a turbo molecular pump. The neutral clusters were produced by the supersonic jet expansion method in the expansion chamber and introduced to an analyzing chamber through a conical skimmer with an aperture of 1 mm. The cluster source with

<sup>a</sup> e-mail: nagaya@scephys.kyoto-u.ac.jp

an alumina cylindrical nozzle, and an inner diameter of  $60\ \mu\text{m}$ , was mounted on a cryostat. The composition, temperature, and pressure of the sample gas were adjusted to control the composition and size of the cluster. In the analyzing chamber, the cluster beam intersected with the X-ray beam ( $3\ \text{mm}$  in width  $\times$   $1\ \text{mm}$  in height for EICO and  $1.5\ \text{mm} \times 0.5\ \text{mm}$  for MHMI) horizontally at right angles. The photoions were forced upward by an entrance electrode, and they passed through a flight tube before reaching a detector. A channeltron was utilized for the EICO. The entrance electrodes and the flight tube formed a Wiley-McLaren type time-of-flight mass spectrometer. The photoelectrons were forced downward and immediately detected by a channeltron. For the EICO measurements, the photoelectron signal delivers a start pulse to a time-to-amplitude converter and the photoion signal delivers a stop pulse, from which the time-of-flight (TOF) of the photoion was determined [11]. For the MHMI measurements, a channeltron detector for ion detection was replaced by a position and time sensitive multi-hit MCP delay-line detector system (RoentDek DLD40 and TDC8). The active detector diameter of the PSD was  $47\ \text{mm}$ . The signals of the photoelectron were used as start signals for the time of flight as in the conventional PE(PI) $_n$ CO measurements [12]. The EICO and MHMI measurements were carried out at photon energies of  $14.08$  and  $14.50\ \text{keV}$ , i.e., on both sides of the krypton K-edge ( $h\nu = 14.326\ \text{keV}$ ).

### 3 Results and discussions

At the beginning of the experiment, we measured the EICO spectrum for an atomic beam of KrAr mixed gas because the neutral cluster jet contains an appreciable amount of uncondensed atoms. The EICO spectrum of the atomic beam shows that the multiple charged ions ( $\text{Kr}^{z+}$ :  $z = 3$  to  $11$ ,  $\text{Ar}^{z+}$ :  $z = 2$  to  $8$ ) are generated as a result of vacancy cascade (auger process and radiative decay). The relative abundance of multiple charged atom is in good agreement with the previous result in literature, [14–17] and the peaks of the singly charged monomer ions ( $\text{Kr}^+$  and  $\text{Ar}^+$ ) were negligible for the atomic beam.

Figure 1 shows the EICO spectra for  $\text{Ar}_{99}\text{Kr}_1$  mixed clusters recorded at photon energies of  $14.08$  and  $14.50\ \text{keV}$ . The average cluster size  $\langle N \rangle$  in Figure 1 was  $100$ . The two major features observed in the EICO spectra of the clusters are as follows: a series peaks due to multiple charged monomer ions below  $2.5\ \mu\text{s}$ , and the peaks due to the singly charged monomer and cluster ions above  $2.7\ \mu\text{s}$ . The widths of the latter peaks are broader than those of the former by a factor of two or more. Narrow peak widths of multiple charged ions suggest the lack of Coulomb explosion for these species. When the X-ray energy is increased from  $14.08\ \text{keV}$  to  $14.50\ \text{keV}$ , the number of  $\text{Ar}^+$  ions clearly increased. This increase in  $\text{Ar}^+$  ion suggests that a charge transfer occurs from the krypton atoms to the argon atoms in the mixed cluster, because only the photoabsorption cross-section of krypton changes remarkably with photon energies near krypton K threshold energy ( $h\nu = 14.326\ \text{keV}$ ).

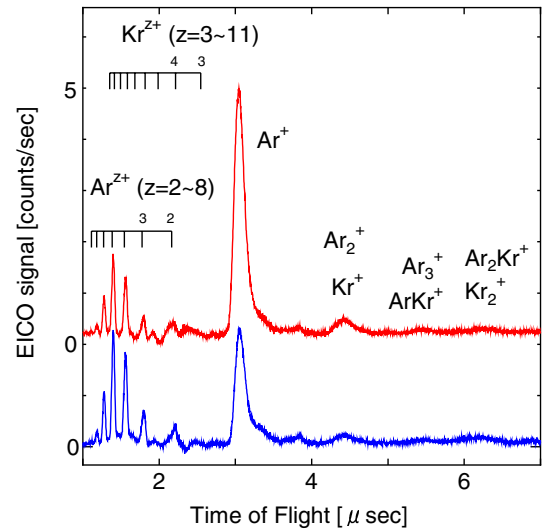


**Fig. 1.** (Color online) EICO spectra for  $\text{Ar}_{99}\text{Kr}_1$  cluster recorded at  $14.50\ \text{keV}$  (upper graph) and  $14.08\ \text{keV}$  (lower graph). Average cluster size  $\langle N \rangle = 100$ .

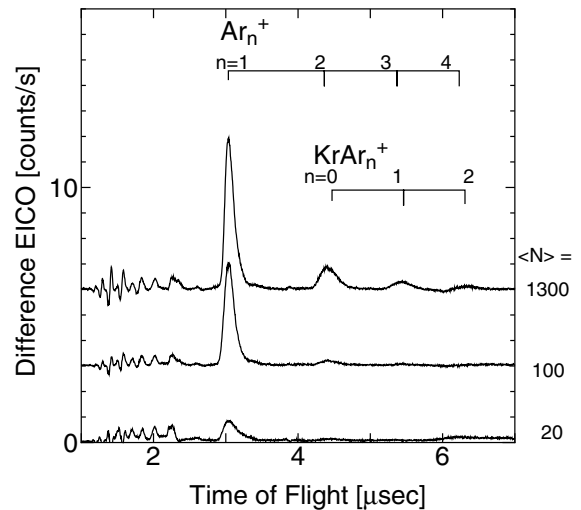


**Fig. 2.** Difference EICO spectra between  $14.08$  and  $14.50\ \text{keV}$  are plotted as a function of time of flight for various cluster size.

In order to estimate the effect of krypton on X-ray absorption, we have extracted the difference EICO, as shown in Figure 2. Here, the difference EICO is defined as the difference of EICO spectra recorded at  $14.08\ \text{keV}$  and  $14.50\ \text{keV}$ . The difference EICO spectra show that the singly charged ions increase dramatically with increasing the average cluster size  $\langle N \rangle$ , and  $\text{Ar}^+$  ions are the dominant species. Present results strongly suggest that the holes created by vacancy cascade on the krypton atoms are transferred to the surrounding atoms before fragmentation, and almost all the resulting ions are singly charged.

Several experimental and theoretical studies have been carried out to investigate the phase separation of mixed rare-gas clusters. Laarmann et al. [18] investigated the energy resolved fluorescence spectra of the mixed rare-gas cluster. They examined the absorption bands caused

by surface exciton and reported that the coexpansion of a dilute ArKr gas mixture results in the penetration of Kr atoms inside Ar clusters. Clarke et al. investigated the phase separation of the binary liquid Lennard-Jones clusters by using both constant temperature Monte Carlo (MC) and constant energy molecular dynamics (MD) method [19]. The cluster morphology was systematically explored by varying the ratios of the Lennard-Jones parameters ( $\epsilon$  and  $\sigma$ ). The results of MD for the ArKr cluster suggest a considerable amount of mixing between the two species and the formation of a Kr core coated by Ar atoms. The difference EICO for  $\langle N \rangle = 1300$  shows that  $\text{Kr}_2^+$  and  $\text{Kr}_3^+$  were hardly generated by the X-ray absorption of krypton. If the Kr atoms tend to coagulate in the mixed clusters,  $\text{Kr}_2^+$  will be generated by the X-ray absorption of krypton for  $\langle N \rangle = 1300$ . The present results suggest that the Kr atoms are surrounded by Ar atoms even in large clusters ( $\langle N \rangle = 1300$ ), which is consistent with the MD results.

The large peak widths of the singly charged ion suggest Coulomb explosion. Let us estimate an upper bound for the charge separation distance (CSD) from the total kinetic energy released by the Coulomb explosion by using the following method. Here, we concentrate on the singly charged ions, because our multi-hit momentum imaging experiment reveals that the multiple charged ions are neither the starting material nor the products of the Coulomb explosion. Since the neutral fragments also obtain their kinetic energy through collisions with ions and/or with other neutral fragments, the total kinetic energy  $K_{\text{ion}}$  of the ionic species, which can be estimated from the EICO spectra, cannot be equated with the total Coulomb energy  $U_{\text{total}}$  stored in the cluster before the Coulomb explosion. Therefore,  $K_{\text{ion}}$  should be treated as a lower bound for  $U_{\text{total}}$ , which gives an upper bound of CSD.

Here, we assume that a sphere with a radius of  $R_0$ , in which the charges  $z_0 e$  are uniformly distributed, is located within a cluster with a radius of  $R_1$ . The total Coulomb energy  $U(R_0)$  may be calculated approximately as

$$U(R_0) = \frac{\epsilon - 1}{2\epsilon} \frac{(z_0 e)^2}{R_1} + \frac{3z_0(z_0 - 1)e^2}{5\epsilon} \frac{1}{R_0} \quad (1)$$

where  $\epsilon$  is the dielectric constant of the cluster relative to that of vacuum, and it is assumed to be the same as that of the bulk material.  $R_1$  can be estimated from  $\langle N \rangle$  by using the bulk density. The above expression is an extension of equation (11) in reference [20] given by Echt et al., who discussed the critical size of a cluster with regard to the electrostatic instability, assuming that the cluster as a whole is uniformly charged. On the other hand, in the present case, the core excitation generates charges that are localized on the atomic scale.

The kinetic energy of each daughter ion  $j$  can be estimated from the half-width  $\Delta t_j$  of the corresponding EICO peak, because  $\Delta t_j$  is related to the velocity  $v_j$  as

$$v_j = \frac{eE}{2m_j} \Delta t_j \quad (2)$$

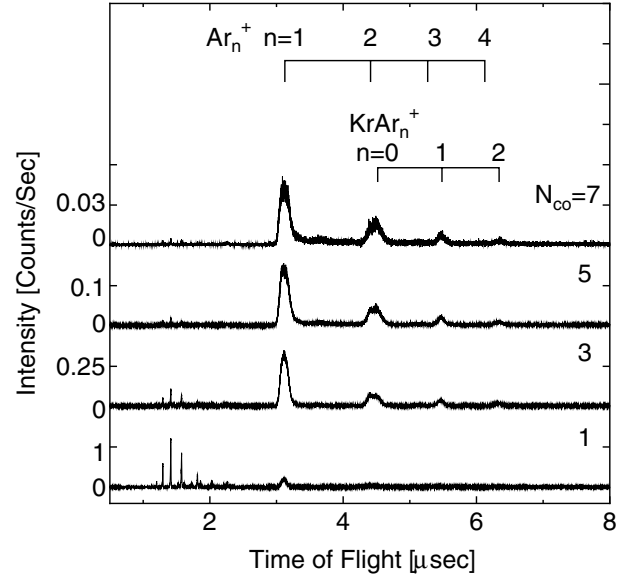


**Fig. 3.** Time-of-flight mass spectra for  $\text{Ar}_{99}\text{Kr}_1$  cluster beams with  $\langle N \rangle = 100$  from MHMI measurements ( $h\nu = 14.50$  keV).  $N_{co}$  means the number of detected ion fragments per parent ion.

where  $E$  is the electric field, and  $m_j$  is the mass of ion  $j$ . The time resolution in the EICO spectrum is corrected for estimating  $v_j$ . The total kinetic energy  $K_{\text{ion}}$  of the ionic species is then expressed as

$$K_{\text{ion}} = z_0 \sum_{j=1} \left( \frac{1}{2} m_j F_j v_j^2 \right) \quad (3)$$

where  $F_j = A_j / \sum_{j=1} A_j$  is the branching ratio of the ions  $j$  produced in the Coulomb explosion. Thus, equating  $U(R_0)$  with  $K_{\text{ion}}$ , one can estimate an upper bound  $R_0^{\text{UB}}$  for  $R_0$ .

The kinetic energy of  $\text{Ar}^+$  estimated from the difference EICO was 4.3 eV for  $\langle N \rangle = 20$  and 1.8–2.1 eV for  $\langle N \rangle \geq 100$ . The corresponding CSD was 6.3 Å for  $\langle N \rangle = 20$  and 9.6 Å for  $\langle N \rangle = 100$ . Considering that the diameter of cluster is about 11 Å for  $\langle N \rangle = 20$ , it is considered that the CSD for  $\langle N \rangle = 20$  reflects the diameter of the cluster. The reason for the kinetic energy being nearly constant for the cluster of  $\langle N \rangle \geq 100$  is that the charges are localized around the X-ray absorbing atoms and the cluster radius is larger than the CSD.

To investigate the details of the Coulomb explosion, MHMI measurements have been carried out for the  $\text{Ar}_{99}\text{Kr}_1$  cluster beam recorded at 14.50 keV. In Figure 3, the multihit data has been classified according to  $N_{co}$ . Here,  $N_{co}$  means the number of detected ion fragments per parent ion.  $N_{co}$  relates to the number of charges generated by an X-ray absorption [13]. The TOF spectra of the multi-hit signals (e.g.,  $N_{co} \geq 3$  in Fig. 3) shows that most of the ion fragments were singly charged ions for  $N_{co} \geq 2$ . Multiple charged ion fragments  $\text{Ar}^{z+}$  ( $z = 2, 3, \dots, 8$ ) and  $\text{Kr}^{z+}$  ( $z = 2, 3, \dots, 11$ ) were hardly

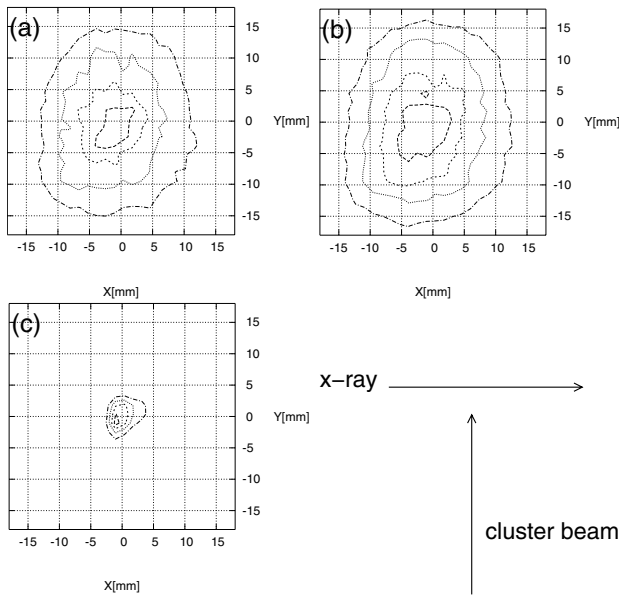


**Fig. 4.** PSD imaging contour maps of  $\text{Ar}^+$  ( $N_{co} = 2$ ) for  $\text{Ar}_{99}\text{Kr}_1$  cluster recorded at (a)  $h\nu = 14.08$  keV and (b) 14.50 keV. Average cluster size was 100. (c) PSD image of atomic beam. Contour interval is 0.2 of the peak height.

detected for  $N_{co} \geq 2$ . Because the multiply charged ions are generated by inner-shell excitation of atomic rare-gases, the present results are evidence of the strong charge migration from the X-ray absorbing atom to the surrounding atoms in the inner-core excited  $\text{ArKr}$  mixed cluster.

The high resolution of the TOF spectra from the MHMI measurements enables us to distinguish between  $\text{Ar}_2^+$  and  $\text{Kr}_1^+$ . It is shown that the peak at  $4.5 \mu\text{s}$  is composed of  $\text{Ar}_2^+$  and  $\text{Kr}_1^+$  while that the peak at  $5.5 \mu\text{s}$  is  $\text{KrAr}^+$  (not  $\text{Ar}_3^+$ ). The frequent decay channel is examined from the multi-hit data. The energy dependence of the multi-hit data reveals that  $(\text{Ar}_1^+ + \text{Ar}_1^+ + \text{Ar}_1^+)$ ,  $(\text{Ar}_1^+ + \text{Ar}_2^+ + \text{Ar}_1^+)$  and  $(\text{Ar}_1^+ + \text{Ar}_1^+ + \text{Kr}_1^+)$  are the frequent decay channel for  $N_{co} = 3$ , resulting from the X-ray absorption of Kr.

Figures 4a and 4b show the space distribution of  $\text{Ar}^+$  ions for  $N_{co} = 2$ . In the case of the atomic beam, the distribution has a sharp peak near the center of the detector  $(X, Y) = (0, 0)$  as shown in Figure 4c. Therefore, the broad distribution of clusters indicates that ion fragments have a large momentum due to Coulomb explosion.

The size of the PSD image recorded at 14.50 keV is about 1.1 times as large as that of 14.08 keV. In the MHMI measurements, the size of the PSD image is proportional to the maximum momentum of the detected ions. Considering that the average charge of the krypton ions increase from 5 to 6 with photon energy [15], the Coulomb repulsive energy among the resulting ions will increase by a factor of 1.2 or more. The large momentum at 14.50 keV may result from the increase in the Coulomb repulsive force in the charged cluster.

## 4 Summary

EICO and MHMI measurements have been carried out for deep inner-core excited mixed rare-gas clusters. The EICO spectra for  $\text{Ar}_{99}\text{Kr}_1$  clusters reveal that the singly charged ions are emitted from the inner-core excited clusters in addition to the multiple charged ions. The dependence of EICO spectra on photon energy and cluster size suggests that holes created by the vacancy cascade on the krypton atom and transferred to surrounding atoms, and that singly charged ions are the primary product of krypton photoabsorption. Charge localization is suggested for the inner-core excited mixed rare-gas clusters from the analysis of the EICO peak width.

The MHMI measurements give us direct evidence for strong charge migration from X-ray absorbing atom to the surrounding atoms. The photon energy dependence of the PSD image for the fragment ions suggests that the momentum of fragment ions depends on the number of charges generated by the vacancy cascade. The present EICO and MHMI results suggest a possibility of the inner-core excitation by hard X-ray for studying the charge dynamics of clusters.

The authors are grateful to Messrs H. Kajikawa and Y. Nishimori for their collaboration in carrying out the experiments. This work is supported by a Grant-in-Aid from the 21st Century COE ‘‘Center for Diversity and Universality in Physics’’ by the Ministry of Education, Culture, Sports, Science and Technology (MEXT) of Japan. This work is also supported by a Grant-in-Aid from Scientific Research by JPSJ (Nos. 12554013, 15651044, 16201021, 18710087).

## References

1. E. Rühl, *Int. J. Mass Spectr.* **229**, 117 (2003)
2. E. Rühl et al., *J. Chem. Phys.* **98**, 6820 (1993)
3. J. Stapelfeldt et al., *Phys. Rev. Lett.* **62**, 98 (1989)
4. R. Feifel et al., *Eur. Phys. J. D* **30**, 343 (2004)
5. M. Lengen et al., *Phys. Rev. Lett.* **68**, 2362 (1992)
6. O. Björneholm et al., *Phys. Rev. Lett.* **74**, 3017 (1995)
7. T. Hayakawa et al., *J. Phys. Soc. Jpn* **69**, 2039 (2000)
8. K. Nagaya et al., *J. Phys. Soc. Jpn* **75**, 114801 (2006)
9. H. Oyanagi et al., *J. Synchrotron Rad.* **6**, 155 (1999)
10. K. Nagaya et al., *Phys. Scripta* **T115**, 984 (2005)
11. J.H.D. Eland, in *Vacuum Ultraviolet Photoionization and Photodissociation of Molecules and Clusters*, edited by C.Y. Ng (World Scientific, Singapore, Teaneck, N.J., 1991), p. 297
12. K. Ueda, J.H.D. Eland, *J. Phys. B* **38**, S839 (2005)
13. H. Iwayama et al., *J. Chem. Phys.* **126**, 024305 (2007)
14. A. Carlson, O. Krause, *Phys. Rev.* **137**, A1655 (1965)
15. O. Krause, T. Carlson, *Phys. Rev.* **158**, 18 (1967)
16. G.B. Armen et al., *Phys. Rev. A* **67**, 42718 (2003)
17. L. Pibida et al., *Nucl. Instrum. Meth. Phys. Res. B* **155**, 43 (1999)
18. T. Laarmann et al., *Surf. Rev. Lett.* **9**, 111 (2002)
19. A.S. Clarke et al., *J. Chem. Phys.* **101**, 2432 (1994)
20. O. Echt et al., *Phys. Rev. A* **38**, 3236 (1988)